

Article

## Optimization of a Finned Shell and Tube Heat Exchanger Using a Multi-Objective Optimization Genetic Algorithm

Heidar Sadeghzadeh <sup>1,\*</sup>, Mehdi Aliehyaei <sup>2</sup> and Marc A. Rosen <sup>3</sup>

<sup>1</sup> Department of Mechanical Engineering, Science and Research Branch, Islamic Azad University, Tehran 1477893855, Iran

<sup>2</sup> Department of Mechanical Engineering, Islamic Azad University, Pardis Branch, Pardis New City, Iran; E-Mail: aliehyaei@yahoo.com

<sup>3</sup> Faculty of Engineering and Applied Science, University of Ontario Institute of Technology, 2000 Simcoe Street North, Oshawa, ON L1H 7K4, Canada; E-Mail: marc.rosen@uoit.ca

\* Author to whom correspondence should be addressed;  
E-Mail: Mechanics\_Sadeghzadeh@yahoo.com; Tel.: +98-914-128-2605.

Academic Editor: Francesco Asdrubali

Received: 30 June 2015 / Accepted: 14 August 2015 / Published: 25 August 2015

---

**Abstract:** Heat transfer rate and cost significantly affect designs of shell and tube heat exchangers. From the viewpoint of engineering, an optimum design is obtained via maximum heat transfer rate and minimum cost. Here, an analysis of a radial, finned, shell and tube heat exchanger is carried out, considering nine design parameters: tube arrangement, tube diameter, tube pitch, tube length, number of tubes, fin height, fin thickness, baffle spacing ratio and number of fins per unit length of tube. The “Delaware modified” technique is used to determine heat transfer coefficients and the shell-side pressure drop. In this technique, the baffle cut is 20 percent and the baffle ratio limits range from 0.2 to 0.4. The optimization of the objective functions (maximum heat transfer rate and minimum total cost) is performed using a non-dominated sorting genetic algorithm (NSGA-II), and compared against a one-objective algorithm, to find the best solutions. The results are depicted as a set of solutions on a Pareto front, and show that the heat transfer rate ranges from 3517 to 7075 kW. Also, the minimum and maximum objective functions are specified, allowing the designer to select the best points among these solutions based on requirements. Additionally, variations of shell-side pressure drop with total cost are depicted, and indicate that the pressure drop ranges from 3.8 to 46.7 kPa.

**Keywords:** finned shell and tube heat exchanger; heat transfer; multi-objective optimization; genetic algorithm; NSGA-II

---

## 1. Introduction

Shell and tube heat exchangers are important components in energy conversion systems, oil and chemical industries, *etc.* In these industries, the heat transfer rate and the total cost of the shell and tube exchangers significantly affect system designs. Extended surfaces (fins) of the shell and tube heat exchangers are applied to enhance heat transfer rates for gas and liquid heat transfer fluids. Fins can be of various geometrical shapes. Generally, fins increase the internal and external tube heat transfer coefficients. Fins are utilized less frequently to decrease shell-side thermal resistance. A suitable and an optimum design, in terms of both economics and efficiency, is obtained through judicious selection of the design parameters.

Research into this topic has been reported previously. Some researchers focused the objective functions on decreasing total cost and heat transfer area [1–3]. Selbas *et al.* [4] optimized a shell and tube heat exchanger economically using a genetic algorithm that considers as the objective function heat transfer area and shows the relationship between heat transfer area and total cost: heat transfer area increases as total cost increases. Vahdat Azad and Amidpour [5] optimized shell and tube heat exchangers based on constructed theory, with the objective of reducing the total cost of the heat exchanger. They use a genetic algorithm to optimize the objective function, which is a mathematical model for the cost of the shell and tube heat exchanger and is based on constructed theory. San and Jan [6] optimized a heat exchanger for waste heat recovery using Second-law optimization. Gupta and Das [7] assessed exergy destruction in a cross-flow configuration analytically, and examined the effects of varying operating parameters and non-uniform flow on the exergetic behavior of cross-flow heat exchangers. Satapathy [8] used second-law analysis to evaluate the thermodynamic irreversibilities for laminar and turbulent flow conditions in a coiled-tube heat exchanger. Sanaye and Haj Abdollahi [9] considered as objective functions (maximum effectiveness and minimum total cost) for a plate fin heat exchanger and chose six decision variables; they use a multi-objective genetic algorithm and depict a set of solutions on a Pareto curve. Najafi *et al.* [10] optimized a plate and fin heat exchanger using genetic algorithm, considering two different objective functions: total heat transfer rate and annual cost. They propose multi-objective optimization as the best way to optimize cases by accounting properly for contradictory objective functions. For their case, increasing heat transfer leads to increased cost (an undesirable state); among the set of solutions, the designer can choose the most desired solution considering limitations related to the project and investment. Haj Abollahi *et al.* [11] reported on the optimization of a compact heat exchanger using a multi-objective genetic algorithm to maximize effectiveness and minimize total pressure drop. When varying decision variables leads to a decrease in pressure drop, effectiveness decreases too. Their Pareto curve indicates the contradictory nature of the two objective functions clearly. Sanaye and Haj Abdollahi [12] used a two-objective optimization genetic algorithm to obtain minimum total cost and maximum heat transfer rate. They introduce a suitable limit on the Pareto curve from cost and efficiency points of view, to assist in the

heat exchanger design. Hilbert [13] used a multi-objective optimizing approach to attain maximum heat transfer rate and minimum pressure drop for a tube bank. Fettaka *et al.* [14] examined multi-objective optimization of a shell and tube heat exchanger using NSGA-II and introduced their objective functions on the basis of heat transfer area and pumping power. They minimized both functions, introduced appropriate continuous and discrete decision parameters, and showed them on a Pareto curve. These curves demonstrate in separate diagrams the impact on heat transfer area of variations in decision variables such as tube length, tube diameter and tube arrangement. Using Delaware's approach, Ponce *et al.* [15] described shell side flow and used a genetic algorithm with a few decision variables to minimize their objective function (total cost), and observed a decrease in pressure drop and total cost compared with a similar analysis in another reference [16]. Munawar and Babu [17] used differential completion for optimizing a shell and tube heat exchanger. They minimized their cost function using seven decision variables including outside diameter of tube, tube pitch, type of shell, number of tube passes, tube length, space of baffles and baffle cut. Caputo *et al.* [18] used the genetic algorithm in Toolbox for optimizing a heat exchanger and considered an objective function on the basis of total cost of the heat exchanger. They minimize the objective function considering decision variables such as tube diameter, shell diameter and space of baffles, and compare their results with traditional approaches. The results indicate an improvement in heat exchanger performance relative to traditional approaches.

The previous studies exhibit some shortcomings. First, there are no studies on finned shell and tube heat exchangers in the context of this article. Second, most prior optimization have single objectives, permitting the use of single-objective optimization and the identification of designs with single solutions. Here, we use two-objective optimization and a set of solutions is obtained. Third, most prior optimizations use the Kern method for calculating the heat transfer coefficient and the shell-side pressure drop, but we used a Simplified Delaware method which has better accuracy than the Kern method. Consequently, the present study investigates the optimization of objective functions using a non-dominated sorting genetic algorithm. The investigation is based on an industrial case, and is performed after modeling the heat flows for a radial low-fin shell and tube heat exchanger and introducing relevant decision variables.

## 2. Mathematical Modeling

The heat transfer rate and thermal effectiveness of a fin heat exchanger type (AES), as shown in Figures 1 and 2, following the TEMA standard can be expressed as follows [19]:

$$q = \varepsilon C_{\min} (T_{h1} - T_{c1}) \quad (1)$$

$$\varepsilon = \frac{2}{(1+c^*) + (1+c^{*2})^{0.5} \coth\left(\frac{NTU}{2}(1+c^{*2})^{0.5}\right)} \quad (2)$$

Here,  $q$  is the heat transfer rate,  $\varepsilon$  is the effectiveness,  $C_{\min}$  is the minimum thermal capacity of the hot and cold fluids (W/K),  $T_{h1}$  and  $T_{c1}$  are the temperatures of the entering hot and cold fluids, respectively,  $C^*$  is the thermal capacity rate and NTU is the number of thermal units. Some of these terms can be evaluated as follows [20]:

$$NTU = \frac{U_o A_{Tot}}{C_{min}} \tag{3}$$

$$C^* = \frac{C_{min}}{C_{max}} = \frac{\min((\dot{m}c_p)_s, (\dot{m}c_p)_t)}{\max((\dot{m}c_p)_s, (\dot{m}c_p)_t)} \tag{4}$$

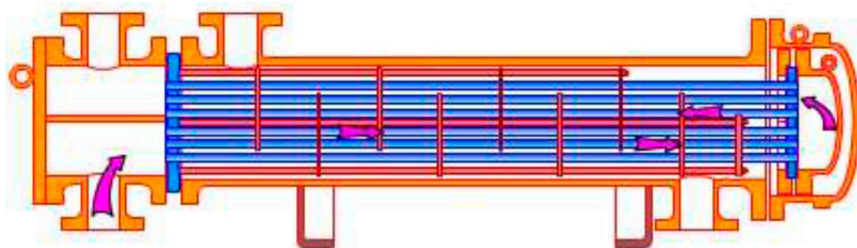


Figure 1. Schematic of shell and tube heat exchanger, type AES [21].

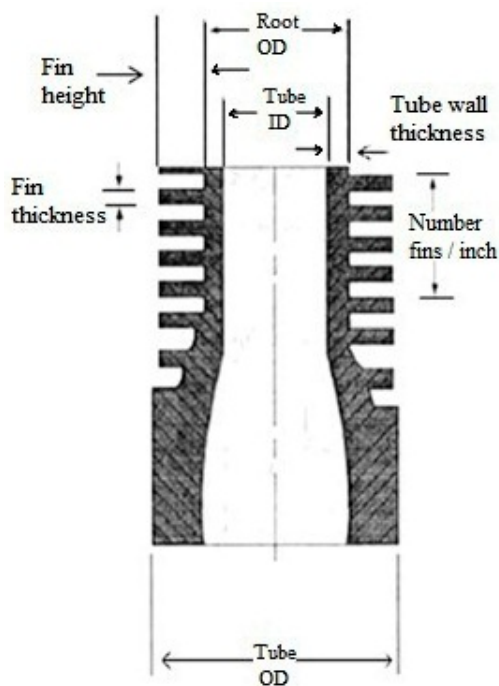


Figure 2. Schematic illustration of a radial low-fin tube [22].

We introduce  $A_{Tot}$  as the total external surface area of a finned tube heat exchanger and  $U_o$  as the overall heat transfer coefficient. These can be expressed as follows [22]:

$$A_{Tot} = A_{fins} + A_{pirim} \tag{5}$$

$$A_{Tot} = [2n_f \pi (r_{2c}^2 - r_1^2) + 2\pi r_1 (1 - n_f \tau)] L N_t \tag{6}$$

$$U_o = \left[ \frac{A_{Tot}}{h_i A_i} + \frac{R_{Di} \cdot A_{Tot}}{A_i} + \frac{A_{Tot} \cdot \ln \frac{d_o}{d_i}}{2\pi \cdot k_{tube} \cdot L} + \frac{1}{h_o \cdot \eta_w} + \frac{R_{Do}}{\eta_w} \right]^{-1} \tag{7}$$

Here,  $L$ ,  $N_t$ ,  $d_i$ ,  $d_o$ ,  $R_{Di}$ ,  $R_{Do}$ ,  $K_w$ ,  $r_{2c}$ ,  $r_1$  and  $n_f$  are tube length, number of tubes, inside and outside diameters of the tube, tube and shell side fouling resistances, thermal conductivity of tube wall,

corrected fin radius, external radius of root tube and number of fins per unit length of tube, respectively. Also,  $A_i$  denotes the internal surface area of the tube, where

$$A_i = \pi d_i L N_t \quad (8)$$

Furthermore,  $\eta_w$  denotes the weighted efficiency of the finned surface, expressible as follows [22,23]:

$$\eta_w = \left( \frac{A_{\text{prim}}}{A_{\text{Tot}}} \right) + \eta_f \left( \frac{A_{\text{fins}}}{A_{\text{Tot}}} \right) \quad (9)$$

and  $\eta_f$  is the fin efficiency:

$$\eta_f = \frac{\tanh(m\psi)}{m\psi} \quad (10)$$

where

$$\psi = (r_{2c} - r_1) \times \left[ 1 + 0.35 \ln \left( \frac{r_{2c}}{r_1} \right) \right] \quad (11)$$

$$m = \left( \frac{2h_o}{K\tau} \right)^{\frac{1}{2}} \quad (12)$$

$$r_{2c} = r_2 + \frac{\tau}{2} \quad (13)$$

In the above relations,  $\Psi$  is a parameter in the equation for efficiency of annular fins,  $\tau$  is the fin thickness and  $k$  is the thermal conductivity.

The fin temperature can be evaluated following the approach described below.

The tube side heat transfer coefficient  $h_i$  is calculated as follows [24–26]:

$$h_i = \left( \frac{k_t}{d_i} \right) 0.116 (\text{Re}_t^{\frac{2}{3}} - 125) \text{Pr}_t^{\frac{1}{3}} \left( 1 + \frac{d_i}{L} \right)^{\frac{2}{3}} \left( \frac{\mu}{\mu_w} \right)^{0.14} \quad \text{for } \text{Re}_t > 10^4 \quad (14)$$

$$h_i = \left( \frac{k_t}{d_i} \right) 0.027 \text{Re}_t^{0.8} \text{Pr}_t^{0.4} \left( \frac{\mu}{\mu_w} \right)^{0.14} \quad \text{for } 2100 < \text{Re}_t < 10^4 \quad (15)$$

$$h_i = \left( \frac{k_t}{d_i} \right) 1.86 \left( \frac{\text{Re}_t \text{Pr}_t d_i}{L} \right)^{\frac{1}{3}} \left( \frac{\mu}{\mu_w} \right)^{0.14} \quad \text{for } \text{Re}_t < 2100 \quad (16)$$

The above equation is acceptable for  $\left( \frac{\text{Re}_t \text{Pr}_t d_i}{L} \right)^{\frac{1}{3}} \times \left( \frac{\mu}{\mu_w} \right)^{0.14} > 2$ , whereas for  $\left( \frac{\text{Re}_t \text{Pr}_t d_i}{L} \right)^{\frac{1}{3}} \times \left( \frac{\mu}{\mu_w} \right)^{0.14} < 2$  the heat transfer coefficient can be expressed as follows [24]:

$$h_i = 3.66 \frac{k_t}{d_i} \quad (17)$$

Here,  $k_t$ ,  $\text{Pr}_t$ ,  $\mu$  and  $\mu_w$  are the tube inside fluid thermal conduction coefficient, the tube side Prandtl number, the viscosity and fluid viscosity evaluated at average temperature of tube wall. Also, the tube side Reynolds number ( $\text{Re}_t$ ) can be evaluated as follows [22]:

$$Re_t = \frac{4 \dot{m}_t \left( \frac{n_p}{N_t} \right)}{\pi \cdot d_i \cdot \mu} \quad (18)$$

where  $\dot{m}_t$  is the mass flow rate and  $n_p$  is the number of tube passes.

The internal tube pressure drop  $\Delta p_t$  includes the pressure drop due to fluid friction in straight sections of tubes  $\Delta p_f$ , the pressure drop due to tube entrance and exit effects  $\Delta p_r$  and the pressure drop in the nozzle  $\Delta p_n$  [22,27,28]. That is,

$$\Delta p_t = \Delta p_f + \Delta p_r + \Delta p_n \quad (19)$$

$$\Delta p_f = f \frac{L \times n_p}{2000 d_i} \frac{G_t^2}{s \left( \frac{\mu}{\mu_w} \right)^{0.14}} \quad (20)$$

$$\Delta p_r = 5 \times 10^{-4} \times \frac{\alpha_r \cdot G_t^2}{s} \quad (21)$$

$$\Delta p_n = 7.5 \times 10^{-4} \times \frac{N_s \cdot G_n^2}{s} \quad \text{for turbulent flow} \quad (22)$$

$$\Delta p_n = 1.5 \times 10^{-3} \times \frac{N_s \cdot G_n^2}{s} \quad \text{for laminar flow} \quad (23)$$

Here,  $G_t$  denotes the shell side mass flux,  $G_n$  the mass flux in the nozzle, and  $N_s$  the number of shells connected in series. Also,  $f$  is the friction coefficient [22]:

$$f = \frac{64}{Re_t} \quad \text{for laminar flow} \quad (24)$$

$$f = 0.4137 Re^{-0.2585} \quad \text{for turbulent flow} \quad (25)$$

$$G_n = \frac{4 \dot{m}}{\pi d_n^2} \quad (26)$$

$$Re_n = \frac{4 \dot{m}_{\text{tube}}}{\pi \cdot d_n \times \mu} \quad (27)$$

Also,  $\alpha_r$  denotes the number of velocity heads allocated for the tube-side minor pressure losses, which can be inferred from Table 1 [22].

**Table 1.** Number of velocity heads allocated for minor losses on tube side.

Flow regime	Regular tubes	U-tubes
Turbulent	$2n_p \cdot 1.5$	$1.6n_p \cdot 1.5$
Laminar, $Re \geq 500$	$3.25n_p \cdot 1.5$	$2.38n_p \cdot 1.5$

The shell diameter is obtained as follows [29]:

$$D_s = 0.637 p_T \sqrt{\pi \times N_t \times \frac{CL}{CTP}} \quad (28)$$

where  $p_T$  is the tube pitch and  $CL$  is the tube arrangement, which equals 1 for 45° and 90° and 0.87 for 30° and 60°. Also,  $CTP$ , which is a tube fixed value, is 0.93, 0.90 and 0.85, respectively for 1, 2 and 3 tube passes.

The Simplified Delaware method is used to calculate the shell-side heat transfer coefficient [22,25]:

$$h_o = j_H \left( \frac{K}{D_e} \right) \times Pr^{\frac{1}{3}} \times \left( \frac{\mu}{\mu_w} \right)^{0.14} \quad (29)$$

where  $J_H$  and  $D_e$  are the modified Colburn factor for the shell-side heat transfer and the equivalent diameter, respectively. These can be evaluated as follows [22,25]:

$$j_H = 0.5 \left( 1 + \frac{B}{ds} \right) \times (0.08 Re_s^{0.6821} + 0.7 Re_s^{0.1772}) \quad (30)$$

For a square pitch,

$$D_e = \frac{4P_T^2 - \pi D_r^{\wedge 2}}{\pi D_r^{\wedge}} \quad (31)$$

and for a triangular pitch,

$$D_e = \frac{4 \times 0.86 P_T^2 - \pi D_r^{\wedge 2}}{\pi D_r^{\wedge}} \quad (32)$$

In above equation,  $D_r^{\wedge}$  is the effective root tube diameter:

$$D_r^{\wedge} = [D_r^2 + 4n_f \times b \times \tau (D_r + b)]^{\frac{1}{2}} \quad (33)$$

where  $D_r$  is the external diameter of the tube root,  $n_f$  is the number of fins per unit length of tube,  $b$  is the fin height, and  $\tau$  is the fin thickness.

In order to calculate the shell-side pressure drop, the Simplified Delaware method is employed, so that the shell-side drop is derived from the friction pressure drop and pressure drop in nozzle [25]. That is,

$$\Delta p_s = \Delta p_f + \Delta p_n \quad (34)$$

$$(\Delta p_f)_{shell} = \frac{f \times G_{shell}^2 \times d_s \times (n_b + 1)}{2000 \times d_e \times s \times \phi} \quad (35)$$

The calculation method for the shell-side pressure drop in the nozzle follows the method for the tube-side pressure drop and employs Equations (22) and (23). In the equation above,  $G_s$  is the shell-side mass velocity [22,25]:

$$G = \frac{\dot{m}_{shell}}{A_s} \quad (36)$$

$$A_s = \frac{d_s CB}{P_T} \quad (37)$$

Here,  $A_s$  denotes flow area across the tube bundle,  $C$  clearance between tubes in the bundle,  $n_b$  number of baffles,  $s$  specific gravity, and  $p_T$  tube pitch (for tube arrangement with  $45^\circ$  using  $\frac{P_T}{\sqrt{2}}$  instead of  $P_T$ ).

The friction coefficient  $f$  can be expressed as follows [22]:

$$f = 144[f_1 - 1.25(1 - \frac{B}{d_s}) \times (f_1 - f_2)] \quad (38)$$

where the terms  $f_1$  and  $f_2$  are determined as explained below. For  $Re_{et} > 1000$ ,

$$f_1 = (0.0076 + 0.000166 \times \frac{d_s}{0.0254}) Re^{-0.125} \quad 0.2032 \leq d_s \leq 1.06 \quad (39)$$

$$f_2 = (0.0016 + 5.8 \times 10^{-5} \times \frac{d_s}{0.0254}) Re^{-0.157} \quad 0.2032 \leq d_s \leq 0.59 \quad (40)$$

and for  $Re_{et} < 1000$ ,

$$f_1 = \exp[0.092(\ln Re)^2 - 1.48 \ln Re - 0.000526(\frac{d_s}{0.0254})^2 + 0.0478 d_s - 0.338] \quad 0.2032 \leq d_s \leq 0.59 \quad (41)$$

$$f_2 = \exp[0.123(\ln Re)^2 - 1.78 \ln Re - 0.00132(\frac{d_s}{0.0254})^2 + 0.0678 \frac{d_s}{0.0254} - 1.34] \quad 0.2032 \leq d_s \leq 0.59 \quad (42)$$

Note that we take  $d_s$  to be 0.59 based on the relationship above for diameters larger than 0.59.

The units for  $f_1$  and  $f_2$  in the above equation are both  $\frac{ft^2}{in^2}$  and  $f$  are dimensionless.

### 3. Genetic Algorithms and Multi-Objective Optimization

The main idea behind evolutionary algorithms was introduced by Rechenberg in 1960 [30]. Genetic algorithms, including branches of these types of algorithms, are computer search methods based on optimizing algorithms and gene and chromosome structures; they were introduced to Holland at Michigan University and developed by students like Goldenberg [31,32]. The general idea of the multi-objective non-dominated sorting genetic algorithm (NSGA) was introduced by Goldenberg in 1989 and then implemented by Deb and Srinvas [33]. An extension of the NSGA algorithm, NSGAI, was proposed by Deb *et al.* [34]. In NSGAI, some solutions for each generation are chosen by the Binary Tournament Selection method. At the first rating, the criterion for selection of a solution is the solution's ranking, and at the second rating, this criterion relates to crowding distance regarding the solution. The lower is the solution ranking and the greater is the crowding distance, the more favorable is the solution. In such an instance,  $b$  is dominated by  $a$ . That is,

$$a \leq b \text{ (a dominated b)} \Leftrightarrow \forall i: a_i \leq b_i \wedge \exists i_o: a_{i_o} < b_{i_o} \quad (43)$$

Also, the crowding distance is as follows, according to Figure 3:

$$d_i^l = \frac{|f_1^{i+1} - f_1^{i-1}|}{f_1^{\max} - f_1^{\min}} \quad (44)$$

$$d_i^2 = \frac{|f_2^{i+1} - f_2^{i-1}|}{f_2^{\max} - f_2^{\min}} \tag{45}$$

$$D = d_i^1 + d_i^2 \tag{46}$$

Here, values of  $f_1^{i+1}$ ,  $f_1^{i-1}$ ,  $f_2^{i+1}$ ,  $f_2^{i-1}$ ,  $f_1^{\min}$ ,  $f_1^{\max}$ ,  $f_2^{\min}$  and  $f_2^{\max}$  are determined in the figure and  $d_i^1$  is the area ratio of the territory at point  $i$  to the total area of objective function  $f_1$ . Also  $d_i^2$  is the area ratio of the same territory point to the total area of objective function  $f_2$  while  $D$  that is the sum of these two ratios, which provides an index of the total territory related to this point and is called the crowding distance.

By repeating the selection of the operator on the population of every generation, a combination of individuals of that generation is chosen to take part in crossover and mutation. The act of crossover occurs on some parts of the set of selected people and the act of mutation is applied on the remaining parts, and this leads to the creation of a child population and mutants, which are merged with the main population. First, members of the created population are sorted in ranking and ascending order. Members of the population with the same rank are sorted on the basis of crowding distance and descending order. At this point, members of the population have been sorted firstly by rank and secondly by crowding distance. The main members of the population are selected from the top of the list equal to the people of the main population and the rest are set aside. The chosen members produce the population of the next generation and this cycle is repeated until the concluding conditions are reached [34,35]. Non-dominated solutions obtained from solving multi-objective optimizing problems are often known as the Pareto front [34]. None of the solutions of the Pareto front is preferred over others and depending on the circumstances we can consider any of them as optimum.

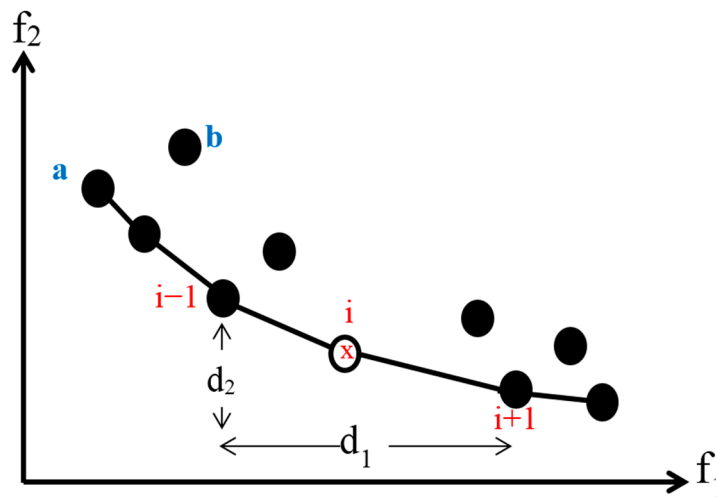


Figure 3. Context of crowding distance for point  $i$ .

#### 4. Objective Functions

Here, the total cost and the heat transfer rate are the two objective functions. The total cost includes initial capital cost and the operating cost includes the pumping cost:

$$C_{\text{total}} = C_{\text{in}} + C_{\text{op}} \tag{47}$$

The operating cost  $C_{op}$  and the initial investment  $C_{in}$  for the shell and the stainless steel tube can be approximated as follows [18,36]:

$$C_{op} = \sum_{k=1}^{n_y} \frac{C_o}{(1+i)^k} \quad (48)$$

$$C_{in} = 8500 + 409A_{Tot}^{0.85} \quad (49)$$

where  $C_o$  is the annual current cost,  $n_y$  lifetime, and  $i$  is the annual inflation rate.

The total operating cost is dependent on the pumping power to overcome the pressure drop from both shell and tube side flow [12,18]:

$$C_o = P \times k_{el} \times H \quad (50)$$

$$P = \left( \frac{\dot{m}_t \Delta P_t}{\rho_t} + \frac{\dot{m}_s \Delta P_s}{\rho_s} \right) \times \frac{1}{\eta} \quad (51)$$

where  $k_{el}$  is the unit price of electrical energy,  $P$  is pumping power;  $H$  is the hours of operation per year and  $\eta$  is the pumping efficiency.

## 5. Case Study

Light oil, for which  $c_p = 2300$  J/kg K, enters the shell of an oil cooler at a temperature of 115.5 °C and a mass flow rate of 44.1 kg/s, while water at a temperature of 29.4 °C and  $c_p = 4186$  J/kg K enters tube of the oil cooler with a mass flow rate of 62.35 kg/s. The applicable conditions are listed in Table 2 [22]. In this case, the equipment life is taken to be  $n_y = 10$  years; the inflation rate is  $i = 10\%$ ; the price of electricity is  $k_{el} = 0.15$  \$/kWh and the working hours and pumping efficiency are  $H = 7500$  h/year,  $\eta = 0.6$ , respectively. The tube arrangement (30°, 45°, 90°), the number of fins per unit length and the diameter (among the 23 available in the TEMA standard listed in Table 3) are three discrete design variables [22]. The bounds for the decision variables (tube arrangement, tube diameter, tube pitch ratio, tube length, numbers of tube, fin height, fin thickness and baffle spacing ratio) involved in optimization of the objective functions (maximum heat transfer rate and minimum total cost) are listed in Table 4.

**Table 2.** Data for the heat exchanger.

Thermophysical and process data	Tube side (water)	Shell side (oil)
Specific gravity (-)	0.99	0.80
Specific heat (J/kg K)	4186	2300
Dynamic viscosity (Pa s)	0.00072	0.00068
Thermal conductivity (W/m K)	0.6404	0.1385
Prandtl number (-)	4.707	11.31
Fouling factor (m <sup>2</sup> W/K)	0.000074	0.00015

**Table 3.** Inner and outer diameters and external diameter of root tube ( $d_i$ ,  $d_o$ ,  $D_r$ ) in inches for 23 standard tubes (for Radial Low-Fin Tubing (Type S/T True fin):19 fins per tube inch).

	$d_i$ (in)	$d_o$ (in)	$D_r$ (in)
1	0.291	1/2	0.375
2	0.384	5/8	0.5
3	0.459	3/4	0.625
4	0.584	7/8	0.75
5	0.709	1.0	0.875
6	0.277	1/2	0.375
7	0.356	5/8	0.5
8	0.495	3/4	0.625
9	0.560	7/8	0.750
10	0.685	1.0	0.875
11	0.259	1/2	0.375
12	0.527	3/4	0.625
13	0.634	7/8	0.75
14	0.759	1.0	0.875
15	0.657	1.0	0.875
16	0.370	5/8	0.5
17	0.509	3/4	0.625
18	0.620	7/8	0.75
19	0.745	1.0	0.875
20	0.402	5/8	0.5
21	0.481	3/4	0.625
22	0.606	7/8	0.75
23	0.731	1.0	0.875

**Table 4.** Bounds for design parameters.

Variable	Lower value (or values considered)	Upper value
Tube arrangement	(30°, 45°, 90°)	-
Tube pitch rate	1.25	2
Tube length (m)	3	8
Tube number	100	700
Baffle spacing ratio	0.2	0.4
Fin height (m)	0.00127	0.003175
Fin thickness (m)	0.000254	0.000304
Number of fins per inch length of tube	(16, 19, 26)	-

## 6. Results of Optimization

In optimizing, the analyst needs to decide which adjustable variables of the problem are more important than others. Here, optimization was implemented using a genetic algorithm for 200 generations with a population of 100 with a crossover probability 0.9 and mutation probability of 0.035. The optimum results are shown on the Pareto curve in Figure 4, which indicates clearly the difference and

conflict between two objective functions, *i.e.*, increasing the heat transfer rate by the heat exchanger leads to an increase in the total cost, and vice versa.

The bounds of the heat transfer rate for this optimization are between 3517 and 7075 kW. The optimization results of the heat transfer rate and the total cost for the four points (A to D) in Figure 4 are listed in Table 5. Point D exhibits the maximum heat transfer rate and the maximum cost, while point A exhibits the minimum for both the cost and the heat transfer rate. If the designer seeks as an objective a high heat transfer rate (without considering cost), point D is a suitable design point, while point A is a suitable design point if low cost (with any value of heat transfer rate) is the intended focus.

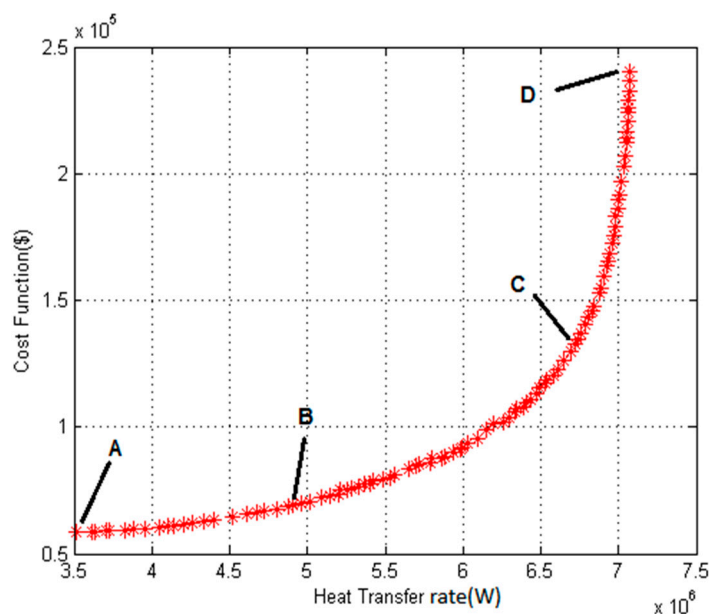


**Figure 4.** The distribution of Pareto-optimal point solutions using NSGA-II.

**Table 5.** Optimized heat transfer rate values and total cost for optimum points A–D on the Pareto front.

	A	B	C	D
Heat transfer rate (kW)	3517	4904	6725	7075
Total cost (\$)	$5.8 \times 10^4$	$6.9 \times 10^4$	$1.3 \times 10^5$	$2.4 \times 10^5$

Choosing optimized points on the Pareto front requires decision making based on an engineering and empirical point of view. Here the results suggest that it is advantageous for the designer to choose design points between (B–C) at which cost function values and heat transfer rate values are both relatively favorable. Correspondingly, the tube arrangement selected for this optimization is 90° and 19 fins per tube inch.

Variations of the shell-side pressure drop with total cost are shown for several optimum points on the Pareto front in Figure 5. The results show that the pressure drop ranges from 3.8 to 46.7 kPa. The pressure drop values attained have high precision due to the use of the Simplified Delaware method.

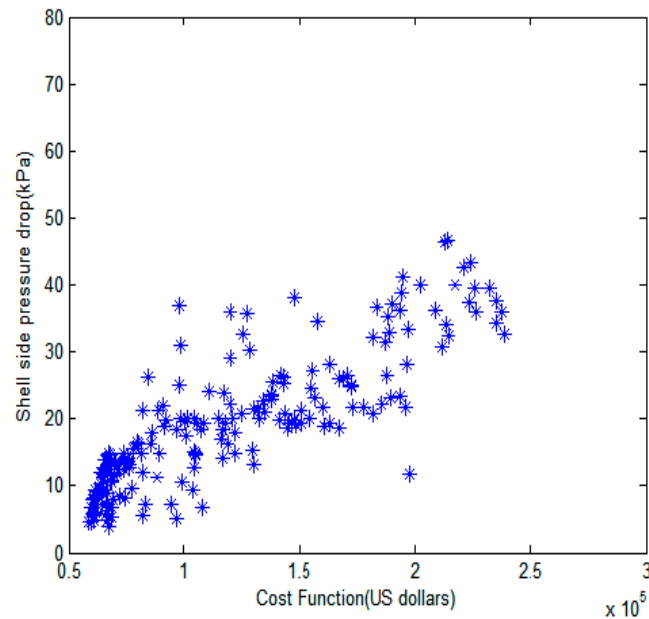


**Figure 5.** Shell side pressure drop (kPa) *versus* the total cost (US dollars).

## 7. Conclusions

The design of a finned shell and tube heat exchanger is successfully optimized using a multi-objective genetic algorithm with the objective functions of maximizing heat transfer rate and minimizing total cost. Nine decision variables are considered, including tube arrangement, tube pitch ratio, number of tubes, tube length, tube diameter, fin height, fin thickness, number of fins per unit length and baffle spacing ratio. A set of solutions is depicted on a Pareto curve and here the best solution bound (from economic and efficiency points of view) is identified among the possible answers on the Pareto front, all of which account for maximum heat transfer rate and minimum cost. The Simplified Delaware method is used for accurately determining the heat transfer coefficients and the shell side pressure drop.

## Author Contributions

Heidar Sadeghzadeh has been done this research with collaboration of Aliehyaei and Professor Rosen. All authors read and approved the final manuscript.

## Conflicts of Interest

The authors declare no conflict of interest.

## Abbreviations

### Nomenclature

$A_i$	Internal surface area of tube ( $m^2$ )
$A_{Tot}$	Total external surface area of a finned tube ( $m^2$ )
$A_s$	Cross flow area at or near the shell centerline ( $m^2$ )
$B$	Baffles spacing (m)
$b$	Fin height (m)

C	Clearance (m)
$C^*$	Heat capacity rate ratio ( $C_h/C_{max}$ )
$C_{in}$	Total investment cost (\$)
CL	Tube layout constant (-)
$C_{max}$	Maximum of $C_h$ and $C_c$ (W/K)
$C_{min}$	Minimum of $C_h$ and $C_c$ (W/K)
$C_o$	Annual operating cost (\$/year)
$C_{op}$	Total operating cost (\$)
$c_p$	Specific heat at constant pressure (J/kg K)
$C_{total}$	Total cost (\$)
CTP	Tube count calculation constant (-)
$D_e$	Equivalent diameter (m)
$d_i$	Tube side inside diameter (m)
$d_n$	Internal diameter of nozzle (m)
$d_o$	Tube side outside diameter (m)
$D_r$	External diameter of tube root (m)
$d_s$	Shell diameter (m)
f	Friction factor (-)
G	Mass flux ( $kg/m^2 \cdot s$ )
H	Hours of operation per year (h/year)
$h_i$	Tube side heat transfer coefficient ( $W/m^2K$ )
$h_o$	Shell side heat transfer coefficient ( $W/m^2K$ )
i	Annual discount rate (%)
$J_H$	Modified Colburn factor for shell-side heat transfer
K	Thermal conductivity (W/m K)
$k_{el}$	Price of electrical energy (\$/kWh)
$L$	Tube length (m)
m	Mass flow rate (kg/s)
$n_b$	Number of baffles (-)
$n_f$	Number of fins per unit length of tube (-)
$n_p$	Number of tube passes (-)
$N_s$	Number of shells connected in series
$N_t$	Number of tubes (-)
NTU	Number of transfer units (-)
$n_y$	Number of baffles (-)
P	Pumping power (W)
$Pr$	Prandtl number (-)
$P_T$	Tube pitch (m)
q	Heat transfer rate (W)
Re	Reynolds number (-)
$R_{Di}$	Fouling resistance shell side ( $m^2 K/W$ )
$R_{Do}$	Fouling resistance shell side ( $m^2 K/W$ )
$r_1$	External radius of root tube (m)
$r_{2c}$	Corrected fin radius (m)
s	Fluid specific gravity (-)
T	Temperature ( $^{\circ}C$ )
U	Overall heat transfer coefficient ( $W/m^2K$ )

**Greek symbols**

$\varepsilon$	Thermal effectiveness (-)
$\Delta p$	Pressure drop (Pa)
$\mu$	Dynamic viscosity (Pa s)
$\eta$	Pump efficiency (-)
$\alpha_r$	Number of velocity heads allocated for tube-side minor pressure losses
$\tau$	Fin thickness (m)
$\rho$	Density (kg/m <sup>3</sup> )

**Subscripts**

F	Fin
i	Inner
o	Outer
s	Shell side
t	Tube side
W	Tube wall

**References**

- Şahin, A.Ş.; Kılıç, B.; Kılıç, U. Design and economic optimization of shell and tube heat exchangers using Artificial Bee Colony (ABC) algorithm. *Energy Convers. Manag.* **2011**, *52*, 3336–3346.
- Costa, A.L.H.; Queiroz, E.M. Design optimization of shell-and-tube heat exchangers. *Appl. Therm. Eng.* **2008**, *28*, 1798–1805.
- Hajabdollahi, H.; Ahmadi, P.; Dincer, I. Thermo-economic optimization of a shell and tube condenser using both genetic algorithm and particle swarm. *Int. J. Refrig.* **2011**, *34*, 1066–1076.
- Selbas, R.; Kızıllan, Ö.; Reppich, M. A new design approach for shell-and-tube heat exchangers using genetic algorithms from economic point of view. *Chem. Eng. Process.* **2006**, *45*, 268–275.
- Vahdat Azad, A.; Amidpour, M. Economic optimization of shell and tube heat exchanger based on constructal theory. *Energy* **2011**, *36*, 1087–1096.
- San, J.Y.; Jan, C.L. Second-law analysis of a wet cross flow heat exchanger. *Energy* **2000**, *25*, 939–955.
- Gupta, A.; Das, S.K. Second law analysis of cross flow heat exchanger in the presence of axial dispersion in one fluid. *Energy* **2007**, *32*, 664–672.
- Satapathy, A.K. Thermodynamic optimization of a coiled tube heat exchanger under constant wall heat flux condition. *Energy* **2009**, *34*, 1122–1126.
- Sanaye, S.; Hajabdollahi, H. Thermal-economic multi-objective optimization of plate fin heat exchanger using genetic algorithm. *Appl. Energy* **2009**, *87*, 1893–1902.
- Najafi, H.; Najafi, B.; Hoseinpoori, P. Energy and cost optimization of a plate and fin heat exchanger using genetic algorithm. *Appl. Therm. Eng.* **2011**, *31*, 1839–1847.
- Hajabdollahi, H.; Tahani, M.; ShojaeFard, M.H. CFD modeling and multi-objective optimization of compact heat exchanger using CAN method. *Appl. Therm. Eng.* **2011**, *31*, 2597–2604.
- Sanaye, S.; Hajabdollahi, H. Multi-objective optimization of shell and tube heat exchangers. *Appl. Therm. Eng.* **2010**, *30*, 1937–1945.

13. Hilbert, R.; Janiga, G.; Baron, R.; Thevenin, D. Multi-objective shape optimization of a heat exchanger using parallel genetic algorithms. *Int. J. Heat Mass Transf.* **2006**, *49*, 2567–2577.
14. Fettaka, S.; Thibault, J.; Gupta, Y. Design of shell-and-tube heat exchangers using multi-objective optimization. *Int. J. Heat Mass Transf.* **2013**, *60*, 343–354.
15. Ponce, J.M.; Serna, M.; Rico, V.; Jimenez, A. Optimal design of shell-and-tube heat exchangers using genetic algorithms. *Comput. Aided Chem. Eng.* **2006**, *21*, 985–990.
16. Mizutani, F.T.; Pessoa, F.L.P.; Queiroz, E.M.; Grossmann, S. Mathematical programming model for heat exchanger network synthesis including detailed heat exchanger designs. *Ind. Eng. Chem. Res.* **2003**, *42*, 4009–4018.
17. Babu, B.V.; Munawar, S.A. Differential evolution for the optimal design of heat exchangers. *Chem. Eng. Sci.* **2007**, *62*, 3720–3739.
18. Caputo, A.C.; Pelagagge, P.M.; Salini, P. Heat exchanger design based on economic optimization. *Appl. Therm. Eng.* **2008**, *28*, 1151–1159.
19. Shah, R.K.; Sekulic, P. *Fundamental of Heat Exchanger Design*; John Wiley & Sons: New York, NY, USA, 2003.
20. Kakac, S.; Liu, H. *Heat Exchangers Selection Rating, and Thermal Design*; CRC Press: New York, NY, USA, 2000.
21. All Free Industrial Ebooks (IE) and Software Downloads. Industrial Training, Mechanical: Heat Exchanger Training. Available online: <http://www.industrial-ebooks.com/> (accessed on 3 October 2013).
22. Serth, R.W. *Process Heat Transfer Principles and Applications*; Academic Press: Kingsville, TX, USA, 2007.
23. McQuiston, F.C.; Tree, D.R. Optimum space envelopes of the finned tube heat transfer surface. *Trans. ASHRAE* **1972**, *78*, 144–152.
24. Seider, E.N.; Tate, C.E. Heat transfer and pressure drop of liquids in tubes. *Ind. Eng. Chem.* **1936**, *28*, 1429–1435.
25. Kern, D.Q.; Krause, A.D. *Extended Surface Heat Transfer*; McGraw-Hill: New York, NY, USA, 1972.
26. Hausen, H. Darstellung des warmueberganges in Rohrendurch Verallgemeinerte Potenzziehungen. *Z.VDI Beih Verfahrenstech* **1943**, *4*, 91–98.
27. Kern, D.Q. *Process Heat Transfer*; McGraw-Hill: New York, NY, USA, 1950.
28. Henry, J.A.R. *Headers, Nozzles and Turnarounds, in Heat Exchanger Design Handbook*; Hemisphere Publishing Corporation: New York, NY, USA, 1988; Volume 2.
29. Taborek, J. Industrial heat exchanger design practices. In *Boiler Evaporators, and Condenser*; John Wiley & Sons: New York, NY, USA, 1991.
30. Rechenberg, I. *Evolutionsstrategie: Optimierung Technischer Systeme Nach Prinzipien der Biologischen Evolution*; Formmann-Holzboog Verlag: Stuttgart, Germany, 1973.
31. Holland, J.H. *Adaptation in Natural and Artificial Systems*; MIT Press: Cambridge, MA, USA, 1992.
32. Goldberg, D.E. *Genetic Algorithms in Search, Optimization, and Machine Learning*; Addison-Wesley: Berkshire, UK, 1989.

33. Srinivas, N.; Deb, K. Multi-objective optimization using non-dominated sorting in genetic algorithms. *J. Evol. Comput.* **1994**, *2*, 221–248.
34. Deb, K.; Agrawal, S.; Pratab, A.; Meyarivan, T. A fast elitist none-dominated sorting in genetic algorithm for multi-objective optimization: NSGA-II. In Proceedings of the Parallel Problem Solving from Nature PPSN VI, Paris, France, 18–20 September 2000.
35. Deb, K.; Pratap, A.; Sameer, A.; Meyarivan, T. A fast elitist multi-objective genetic algorithm: NSGA-II. *IEEE Trans. Evolut. Comput.* **2008**, *6*, 182–197.
36. Taal, M.; Bulatov, I.; Klemes, J.; Stehlik, P. Cost estimation and energy price forecasts for economic evaluation of retrofit projects. *Appl. Therm. Eng.* **2003**, *23*, 1819–1835.

© 2015 by the authors; licensee MDPI, Basel, Switzerland. This article is an open access article distributed under the terms and conditions of the Creative Commons Attribution license (<http://creativecommons.org/licenses/by/4.0/>).